The battle against antimicrobial resistant bacterial infections: next stage development of antimicrobial peptides

Gent, M.E. van

5

Encapsulation into hyaluronic acid-based nanogels improves the selectivity index of the snake cathelicidin Ab-Cath

Miriam E. van Gent, Sylvia N. Kłodzińska, Maureen Severin, Muhanad Ali, Bjorn R. van Doodewaerd, Erik Bos, Roman I. Koning, Jan Wouter Drijfhout, Hanne M. Nielsen and Peter H. Nibbering

Submitted

Abstract

The antimicrobial peptide Ab-Cath, is a promising candidate for development as treatment for antimicrobial resistant (AMR) bacterial infections. Future clinical use is hampered by Ab-Cath's cationic peptidic nature and limited therapeutic window. Here, we evaluated hyaluronic acid-based nanogels for encapsulation of Ab-Cath to circumvent these limitations. Using microfluidics, monodispersed anionic nanogels of 156-232 nm encapsulating >99% Ab-Cath were prepared. Unprecedented, lyophilization using polyvinyl alcohol and dextran-40 provided Ab-Cath nanogel protection and allowed easy dose adjustment. Lyophilized and redispersed Ab-Cath nanogels were as effective as Ab-Cath solution in killing AMR *Staphylococcus aureus*, *Acinetobacter baumannii* and *Escherichia coli* in biological fluids, and in reducing *S. aureus* and *A. baumannii* biofilms. Importantly, encapsulation of Ab-Cath in nanogels reduced Ab-Cath's cytotoxic effects on human fibroblasts by ≥10-fold. Moreover, cutaneous application of Ab-Cath nanogels eliminated bacteria colonizing 3D human skin. These findings affirm the use of nanogels to increase the selectivity index of antimicrobial peptides.

Highlights

- Ab-Cath is a snake-derived cathelicidin with good antibacterial activities
- Encapsulation in OSA-HA nanogels doesn't affect Ab-Cath's antibacterial activities
- Encapsulation in OSA-HA nanogels reduces Ab-Cath's cytotoxicity
- PVA and dextran-40 protect Ab-Cath nanogels during lyophilization

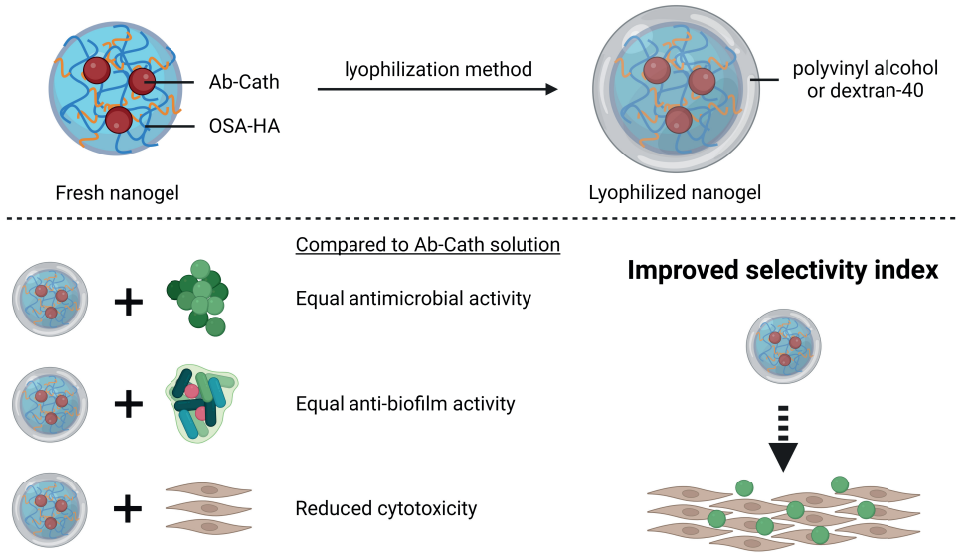

Graphical abstract

1. Introduction

Chronic wound infections are responsible for considerable morbidity and significantly contribute to the high cost of health care. The majority of these infections are caused by *Staphylococcus aureus*, however most often chronic wound infections are polymicrobial, where two or more species of Gram-positive and/or Gram-negative bacteria occupy the infection site [1, 2]. Usually, these infections are accompanied with formation of biofilms, i.e. complex structures of bacteria and their self-produced molecules, such as extracellular polymeric substances [3]. Biofilm-residing bacteria are 10-1000 times more resistant to antibiotics compared to their planktonic counterparts [3, 4]. This, in combination with the rising numbers of antimicrobial resistance worldwide emphasizes the urgent need for novel broad-spectrum antimicrobial agents as alternatives to current antibiotics. Antimicrobial peptides (AMPs) may fulfil this role.

A candidate AMP is Ab-Cath, that belongs to the family of cathelicidins. This peptide's sequence was mined from the genome of the snake *Anilos bitubercalatus*. Ab-Cath is an amphipathic peptide spanning 32 amino acids and is considerably cationic. The peptide is highly effective against antimicrobial resistant (AMR) bacteria and, in particular, against Gram-negative strains (Voet and Nibbering, personal communication). Importantly, Ab-Cath maintains bactericidal effects against bacteria in plasma and whole blood, though its accompanying moderate cytotoxicity to mammalian cells may challenge its development into a therapeutic dosage form.

One strategy to improve the therapeutic potential of Ab-Cath is encapsulation of the peptide into a drug delivery system composed of biodegradable and biocompatible polymers, such as hyaluronic acid (HA), which has antiadhesive and antibiofilm properties towards bacteria [5]. HA may be modified with octenyl succinic anhydride (OSA) to produce a polymer with amphiphilic properties [6], allowing the polymer to self-assemble into soft flexible nanogels composed of hydrophobic and hydrophilic zones within the nanogel matrix [7, 8]. Nanogels composed of OSA-HA reduced the cytotoxicity of a range of molecules, including AMPs [9], peptidomimetics [10], and antibiofilm peptides [11]. These nanogel formulations are produced as aqueous dispersions by using microfluidics-assisted self-assembly, yet the nanogels and the encapsulated peptides typically display limited shelf-lives under this condition [12]. Lyophilization of nanogels is commonly applied to improve drug formulation stability, long-term storage, product shelf-life, and to ease distribution [13]. Development of a lyophilization method is therefore essential for translation of Ab-Cath nanogels to the clinic.

In this study, we aimed to formulate Ab-Cath in OSA-HA nanogels to reduce cytotoxicity while maintaining the antimicrobial activity of Ab-Cath, i.e. to increase the peptide's selectivity index. Moreover, an effective lyophilization method was developed allowing for prolonged storage and concentration of the nanogels.

2. Materials and methods

2.1. Materials

Hyaluronic acid (HyaCare, 50 kDa) was purchased from Evonik Nutrition and Care (Essen, Germany). Octenyl succinic anhydride (OSA, 97%), lysozyme egg white, D-mannitol (≥98%), trifluoroacetic acid (TFA), Triton™ X-100 and bovine serum albumin (BSA) were obtained from Sigma-Aldrich (St. Louis, MO, USA). Sodium bicarbonate ($NaHCO_3$), sodium hydroxide (NaOH), calcium chloride ($CaCl_2$) and human serum (male, type AB) were obtained from Merck (Darmstadt, Germany). Ab-Cath (acetyl-KRFKKFFRKVKKGVHRYFKKNKFYIAATIPYYG-amide; 4159.6 g/mol) was purchased from Enzypep (Geleen, Netherlands) with >98% purity. Lyophilized Ab-Cath was stored at -20°C until use. Polyvinyl alcohol (PVA) was purchased from Acros Organics (Geel, Belgium) and dextran-40 was a kind gift from Avivia (Nijmegen, Netherlands). Uranyl acetate (UA) was obtained from Fluka (Charlotte, NC, USA). Analytical grade solvents for UPLC analysis included ultrapure water (Veolia Purelab Chorus 1, High Wycombe, UK) and acetonitrile (100%, VWR, PA, USA). Ultrapure water was obtained from a MilliPore system (Merck), and phosphate buffered saline (PBS) from Fresenius Kabi (Graz, Austria). Tryptic soy broth (TSB), brain heart infusion (BHI) and Mueller-Hinton (MH) agar were purchased from Oxoid (Basingstoke, UK). Human plasma was obtained from Sanquin (Leiden, Netherlands). Dulbecco's Modified Eagle Medium (DMEM) supplemented with 1% (v/v) GlutaMAX™, penicillin-streptomycin (pen/strep) and trypsin-EDTA were obtained from Gibco (Waltham, MA, USA). Microplates were purchased from Greiner BioOne (Alphen a/d Rijn, Netherlands) and culture plates and inactivated fetal bovine serum (FBSi) from Corning (NY, USA).

2.2. Modification of hyaluronic acid with octenyl succinic anhydride

Octenyl succinic anhydride-modified hyaluronic acid (OSA-HA, 17%-32% degree of substitution, see **Figures S1-3**) was synthesized as described by Eenschoten et. al [6]. Briefly, 1.25 g HA was dissolved into 50 mL ultrapure water and $NaHCO_3$ was added to yield a 2 M carbonate solution. Afterwards the pH was adjusted to pH 8.5 with 0.5 M NaOH and OSA was added dropwise to the HA solution to reach a 50:1 molar ratio of OSA:HA. The solution was left to react overnight at room temperature. Then, the reaction product was dialyzed against ultrapure water at 4 °C with water refreshment regularly until the conductivity reached a value lower than 5 µS/cm.

Finally, the produced OSA-HA was lyophilized and characterized with ^{1}H-NMR.

2.3. Preparation of Ab-Cath OSA-HA nanogels

Ab-Cath OSA-HA nanogels were produced at room temperature using a microfluidic chip design previously described [14]. Ab-Cath and OSA-HA were dissolved in ultrapure water to a concentration of 1500 µg/mL (10× final peptide concentration) and 500 µg/mL, respectively. The solutions were filled into 3 gastight fixed Luer lock tip glass syringes (Prosense, Oosterhout, Netherlands) mounted on 3 NE-300 syringe pumps (Prosense) to be able to control the flow rates. The OSA-HA solution was injected into the outer streams of the microfluidic chip at a flow rate of 0.99 mL/min and the peptide solution was injected into the middle stream at a flow rate of 0.22 mL/min, resulting a combined flow of 2.2 mL/min. The produced nanogels contained 150 µg/mL Ab-Cath and 500 µg/mL OSA-HA. For the experiments either freshly prepared nanogels or lyophilized nanogels were used; the concentration of peptide is given as the total peptide concentration present in the sample. Freshly prepared nanogels were stored at 4 °C and used within one week. For lyophilization of nanogels, cryoprotectant solutions containing 1-50 mg/mL D-mannitol, dextran-40 or PVA were added in a 1:1 (v/v) ratio to the nanogels, and the nanogel solution was lyophilized overnight using an Alpha 1-4 LSCbasic freeze dryer (Martin Christ Gefriertrocknungsanlagen, Osterode am Harz, Germany) with RV3 vacuum pump and EMF10 oil mist filter (Edwards, Burgers Hill, UK). Freshly prepared nanogels were diluted, and lyophilized nanogels resuspended, into the relevant media before use.

2.4. Size, polydispersity index and zeta potential of the nanogels

Dynamic light scattering was used to determine the average nanogel size and polydispersity index (PDI), while the surface charge of the nanogels was estimated by the zeta potential (ZP). The size, PDI and ZP measurements were performed in ultrapure water at 25 °C using a Zetasizer Nano ZS (Malvern Instruments, Worcestershire, UK) equipped with a 633 nm laser and 173° detection optics. Malvern DTS v.6.20 software was used for data acquisition and analysis. Measurements were performed for 3 independent sample batch replicates.

2.5. Transmission electron microscopy

Nanogels were visualized using negative stain transmission electron microscopy (TEM). Briefly, 200 mesh formvar and carbon coated copper EM grids (Agar Scientific, Stansted, UK) were glow-discharged by 0.2 mbar air for 1 min using the glow discharger unit of an EMITECH K950X (Quorum Technologies, Lewes, UK). Then, 3 µL of nanogel (containing 150 µg/mL Ab-Cath and 500 µg/mL OSA-HA) was applied per glow-discharged grid for 1 min and the grids were blotted to remove

excess of sample. Subsequently, the grids were stained on droplets of 2% (w/v) UA in water for 1 min, after which excess of the staining solution was removed with blotting paper. Imaging of the air-dried grids was performed at 120 kV on a Tecnai 12 electron microscope (ThermoFisher, Waltham, MA, USA). A 4k×4k Eagle camera (ThermoFisher) was used to record images at 11,000× magnification.

2.6. Quantification of Ab-Cath

Quantification of Ab-Cath was performed using an ACQUITY H-class UPLC-MS system (Waters, Milford, MA, USA) with an LCT-premier mass detector (Waters). Chromatographic separation was carried out on an ACQUITY UPLC BEH C18 column (100 x 2.1 mm, 1.7 µm; Waters). The mobile phase consisted of eluent A (100% water) and eluent B (100% acetonitrile), both containing 0.05% (v/v) TFA. Samples were run with a gradient of 5 to 75% eluent B over 8 min at 0.5 mL/min at 50 °C. The data were analyzed using MassLynx Software V4.2 and a calibration curve of Ab-Cath (0.01-0.1 mg/mL).

2.7. Encapsulation of Ab-Cath into OSA-HA nanogels

The Ab-Cath amount encapsulated in nanogels was determined indirectly by measuring the residual amount of peptide present in the aqueous bulk phase after nanogel production. The aqueous bulk phase was obtained by centrifuging the nanogels at 500,000 × g for 30 min. The encapsulation efficiency (EE) was quantified for 3 independent sample batch replicates. Calculations of the EE are based on the theoretical amount of Ab-Cath encapsulated, as only non-encapsulated Ab-Cath was measured:

$$EE\ (\%) = \frac{Total\ Ab-Cath\ (\mu g) - unencapsulated\ Ab-Cath\ (\mu g)}{Total\ Ab-Cath\ (\mu g)} * 100\% \quad (1)$$

Similarly, the drug loading (DL) was calculated:

$$DL\ (\%) = \frac{Encapsulated\ Ab-Cath\ (\mu g)}{Total\ weight\ nanogels\ (\mu g)} * 100\% \quad (2)$$

2.8. Release of Ab-Cath from nanogels

In vitro release studies with lyophilized Ab-Cath nanogels were performed in PBS using dialysis membranes (Spectra-Por® Float-a-Lyzer® G2, MWCO 100 kDa, Spectrum Labs, Breda, Netherlands). Prior to use, dialysis membranes were washed according to manufacturer's protocol. Next, dialysis membranes were coated with 1 mg/mL lysozyme egg white for 1 h at 37 °C and 200 rpm using an orbital shaker. Dialysis membranes were then washed with ultrapure water and loaded with 1 mL of Ab-Cath or Ab-Cath nanogels (at 300 µg/mL) and placed in 6 mL of release buffer while continuously shaking at 200 rpm. Temperature was maintained at

37 °C throughout the experiment and 1 mL samples were taken until 5 h, replacing sample volumes with equal volumes of PBS. From 5 h onwards, 6 mL samples were taken to maintain sink conditions. Samples were stored at -20 °C until analysis by UPLC. Results are expressed as percentage of Ab-Cath released from the nanogels compared to Ab-Cath solution.

2.9. Bacterial strains and culturing

Antimicrobial-resistant (AMR) strains used in this study include *Acinetobacter baumannii* strain (RUH875), methicillin-resistant *Staphylococcus aureus* (MRSA) strain LUH14616 (NCCB100829) and *Escherichia coli* strain LUH15174 (SPA012, invasive strain). Bacteria were stored in glycerol at -80 °C util use. In short, bacteria were cultured on blood agar plates overnight at 37 °C. Next, 3-5 colonies were cultured to mid-log phase in TSB for 2.5 h under continuous rotation. Mid-log phase bacteria were centrifuged at 1,000 × g for 10 min, washed with PBS and resuspended in the preferred medium to the required concentrations based on the optical density at 600 nm.

2.10. *In vitro* killing assay

Mid-log phase bacteria were resuspended in PBS to a concentration of 5×10^6 colony forming units (CFU)/mL. Subsequently, 30 µL of PBS containing increasing concentrations of Ab-Cath, Ab-Cath nanogels or placebo nanogels, 50 µL of pooled human plasma (Sanquin) or human urine (healthy volunteers) and 20 µL of the bacterial suspension were pipetted into wells of a polypropylene V-shaped microplate. After incubation for 4 h at 37 °C under rotation at 200 rpm, the number of viable bacteria was assessed microbiologically. Results are expressed as lethal concentration $(LC)_{99.9}$, i.e. the lowest concentration of Ab-Cath killing 99.9% of the inoculum.

2.11. *In vitro* biofilm breakdown assay

Mid-log phase bacteria were diluted in BHI to grow 24 h biofilms. Briefly, 100 µL of mid-log phase bacteria at 1×10^7 CFU/mL was added to each well of a polypropylene flat-bottom microplate and incubated for 24 h at 37 °C in humidified environment. The next day, planktonic bacteria were removed from the wells and biofilms were washed twice with 100 µL of PBS to remove remaining non-adherent bacteria. Biofilms were subsequently exposed to increasing concentrations of Ab-Cath, Ab-Cath nanogels, or placebo nanogels in PBS for 4 h at 37°C. Plates were sealed with AmpliStar Adhesive Plate Seals (Westburg, Leusden, Netherlands). Medium controls were checked for possible contamination. Finally, biofilms were washed twice with PBS and biofilm-residing bacteria were harvested by sonication (Branson 1800 sonicator, 10 min) in 100 µL of PBS. The number of viable bacteria was assessed microbiologically.

Results are expressed as the biofilm eradication concentration $(BEC)_{99.9}$, i.e. the lowest concentration of Ab-Cath killing 99.9% of the bacteria in the biofilm.

2.12. *In vitro* cytotoxicity assay using human primary skin fibroblasts

Human primary skin fibroblasts (kindly provided by dr. A. El Ghalbzouri, Department of Dermatology, LUMC) were grown in culture flasks using DMEM supplemented with 1% (v/v) GlutaMAX™, 1% (v/v) pen/strep and 5% (v/v) FBSi. Fibroblasts were harvested using 0.05% (v/v) trypsin-EDTA, washed and resuspended to 2×10^5 cells/mL and finally 20,000 cells were seeded in 96-wells flat-bottom culture plates. Monolayers developed overnight at 37 °C and 5% CO_2 and were exposed for 4 h to increasing concentrations of Ab-Cath, lyophilized and redispersed Ab-Cath nanogels and placebo nanogels in DMEM supplemented with GlutaMAX™, 1% (v/v) pen/strep and 0.5% (v/v) human serum. 1% (v/v) Triton™ X-100 and medium were included as positive and negative control, respectively. Lactate dehydrogenase (LDH) release into the supernatants was detected by the Cytotoxicity Detection Kit (Roche, Basel, Switzerland) and the metabolic activity of the cells was measured using cell proliferation reagent WST-1 (Roche), both according to manufacturer's instructions. Results are expressed as effective concentration $(EC)_{50}$, i.e. the highest concentration of Ab-Cath inducing 50% reduction of cytotoxicity or metabolic activity. Non-linear regression curves with bottom and top restrictions at 0 and 100% were fitted for each individual experiment to determine medians (and ranges) of the EC_{50} values.

2.13. Calculation of the selectivity index

The selectivity index, i.e. ratio between cytotoxicity and bactericidal activity, was calculated as follows:

$$Selecitivity\ index = \frac{Cytotoxicity\ (\mu M)}{Bactericidal\ activity\ (\mu M)} \quad (3)$$

2.14. 3D human skin equivalents

Human skin equivalents (HSEs) were cultured using Ker-CT cells (ATCC® CRL-4048™) as described previously [15]. At least 2 days before infection, the culture medium was replaced by culture medium without antibiotics. The HSEs were inoculated with AMR *S. aureus* LUH14616 or *A. baumannii* RUH875 at a concentration of 1×10^5 CFU/model for 1 h at 37 °C and 5% CO_2. After inoculation, the bacterial suspension was removed, the cells were washed with PBS and the colonized models were treated with Ab-Cath, lyophilized and redispersed Ab-Cath nanogels or placebo nanogels at the desired concentrations in PBS for 4 h after which the supernatants (non-adherent bacteria) were stored on ice, while the models (adherent bacteria) were homogenized (5000 rpm, 3×10 s, 10 s pause) using a

bead-beater (Precellys 24 lysis and homogenization, Bertin Technologies). Bacterial counts in both fractions were assessed microbiologically. Results are expressed as individual values and medians of 3 individual measurements performed in duplicate.

2.15. *In vitro* cytotoxicity towards 3D human skin equivalents

HSEs, cultured as described earlier, were exposed to Ab-Cath, lyophilized and redispersed Ab-Cath nanogels or placebo nanogels at the desired concentrations in PBS for 4 h including 1% (v/v) Triton™ X-100 as positive control and PBS as negative control. Afterwards, LDH release from dead cells into the super- and subnatants was detected by the Cytotoxicity Detection Kit (Roche, Basel, Switzerland) according to manufacturer's instructions. Models were cut out, transferred to 24 well flat-bottom culture plates (Corning, NY, USA) and exposed to WST-1 reagent (Cell proliferation reagent WST-1; Roche) in Dulbecco′s Modified Eagle′s Medium (DMEM) medium (Gibco, Waltham, MA, USA) overnight to determine the metabolic activity of the cells in the models. Read-out of medium solutions without the models was performed according to manufacturer's protocol. Results are expressed as percentage cytotoxicity or metabolic activity relative to the controls.

2.16. Statistics

Differences between 2 groups (Ab-Cath, Ab-Cath nanogels or placebo nanogels) were evaluated by a Kruskal-Wallis test, followed by a Mann-Whitney rank sum test using Graphpad Prism software version 6.0 (Graph Pad Software). Differences were considered statistically significant when $p<0.05$.

3. Results

3.1. Physicochemical properties of freshly produced Ab-Cath nanogels

Ab-Cath OSA-HA nanogels were prepared using increasing concentrations of Ab-Cath at a peptide to polymer ratio of 0.3:1 (w/w). Produced nanogels ranged in size from 195 nm to 465 nm; all being monodisperse, negatively charged, and with high encapsulation efficiency and drug loading (**Table 1**). Incorporation of increasing amounts of Ab-Cath resulted in less negatively charged nanogels and increased

Table 1. Physicochemical properties of freshly produced OSA-HA nanogels prepared with increasing Ab-Cath concentrations.

Ab-Cath (µg/mL)	OSA-HA (µg/mL)	Size (nm)	PDI	ZP (mV)	EE (%)	DL (%)
0	500	238 ± 25	0.15 ± 0.06	-32.6 ± 2.7	-	-
150	500	194 ± 38	0.06 ± 0.04	-16.5 ± 3.1	99.7 ± 0.1	23
200	666.7	367 ± 160	0.06 ± 0.04	-14.3 ± 6.4	99.7 ± 0.1	23
250	833.3	465 ± 163	0.06 ± 0.05	-11.4 ± 1.6	99.6 ± 0.1	23

Data are presented as mean ± SD of 3-24 independent sample batch replicates. OSA-HA = octenyl succinic anhydride-modified hyaluronic acid; PDI = polydispersity index; ZP = zeta potential; EE = encapsulation efficiency; DL = drug loading.

nanogel sizes. OSA-HA nanogels containing 150 µg/mL Ab-Cath were chosen for further evaluation, considering a preferred particle size between 150-200 nm [16, 17].

3.2. Stability of freshly produced Ab-Cath nanogels during storage

The physicochemical properties of OSA-HA nanogels were monitored over a 15-day period to determine the colloidal stability of the nanogels in ultrapure water stored at 4 °C. Results showed no significant ($p>0.05$) differences in size, PDI and ZP for both Ab-Cath and placebo nanogels during storage (**Figure 1**). Therefore, OSA-HA nanogels were considered physically stable over this period.

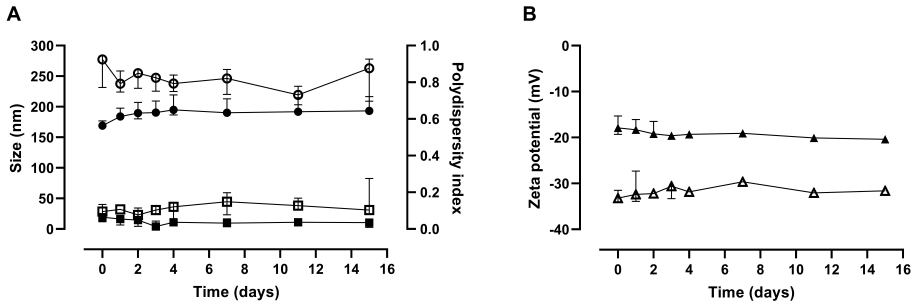

Figure 1. Stability of Ab-Cath (solid) and placebo (open) OSA-HA nanogels over time. (a) size (circle) and polydispersity index (square) and (b) zeta potential. Data are presented as median and error of 3 independent sample batches, with the exception of zeta potential data from day 4 onwards that are data of 2 independent sample batches.

3.3. Antimicrobial activity of freshly produced Ab-Cath nanogels

Next, we compared the antimicrobial activity of Ab-Cath nanogels to Ab-Cath and, as control, placebo nanogels on AMR *S. aureus* and *A. baumannii* in 50% (v/v) plasma and *E. coli* in 50% (v/v) urine. After 4 h, 24 h and 48 h of exposure, the bactericidal activity of Ab-Cath nanogels was similar to Ab-Cath (**Table 2**). Placebo nanogels did not show any bactericidal activity at the tested concentrations.

Table 2. *In vitro* time-killing activities of freshly produced Ab-Cath nanogels.

Species	Strain	Exposure	$LC_{99.9}$ (µM) Ab-Cath	Ab-Cath nanogel	Placebo nanogel
S. aureus	LUH14616	4 h	**1.6** (1.6-3.2)	**1.6** (1.6-3.2)	**>12.8**
		24 h	**0.8** (0.8-3.2)	**0.8** (0.8-3.2)	**>12.8**
		48 h	**1.6**	**3.2** (0.8-6.4)	**>12.8**
A. baumannii	RUH875	4 h	**0.2** (0.1-0.4)	**0.4** (0.2-0.4)	**>6.4**
		24 h	**0.1**	**0.2** (0.05-0.2)	**>6.4**
		48 h	**0.2**	**0.4** (0.2-0.4)	**>6.4**
E. coli	LUH15174	4 h	**0.8** (0.4-1.6)	**0.8** (0.4-1.6)	**>3.2**

Bactericidal activity on AMR bacteria upon 4 h, 24 h and 48 h exposure to increasing concentrations of Ab-Cath, Ab-Cath nanogels and placebo nanogels in 50% (v/v) plasma (*S. aureus* and *A. baumannii*) or 50% (v/v) urine (*E. coli*) was assessed. Results are expressed as median and ranges of 2-4 independent experiments performed in duplicate and is shown as $LC_{99.9}$, i.e. the lowest concentration of peptide to kill 99.9% of the bacteria.

3.4. Physicochemical properties of lyophilized Ab-Cath nanogels

Lyophilization was applied to allow further testing of more concentrated Ab-Cath nanogels, i.e. antibiofilm and cytotoxic activities. As this process could potentially destabilize the nanogels, the ability of various cryoprotectants to protect the nanogels during lyophilization was investigated. TEM microscopical examination of fresh Ab-Cath nanogels revealed individual spherical nanogels with a monodisperse size distribution (**Figure 2a**), whereas collapsed nanogels and aggregates were seen after lyophilization without cryoprotectants (**Figure 2b**). Lyophilization of Ab-Cath nanogels in presence of 10 mg/mL PVA (**Figure 2c**) and 10 mg/mL dextran-40 (**Figure 2d**), but not 50 mg/mL mannitol (**Figure 2e**), maintained the morphology of the nanogels. Further investigations revealed no major differences in size, PDI and ZP between lyophilization without cryoprotectants and lyophilization in presence of PVA, dextran-40 or mannitol (**Table 3**). Use of mannitol was restricted due to its low solubility. Together, these data indicate that both PVA and dextran-40 protect Ab-Cath nanogels during lyophilization.

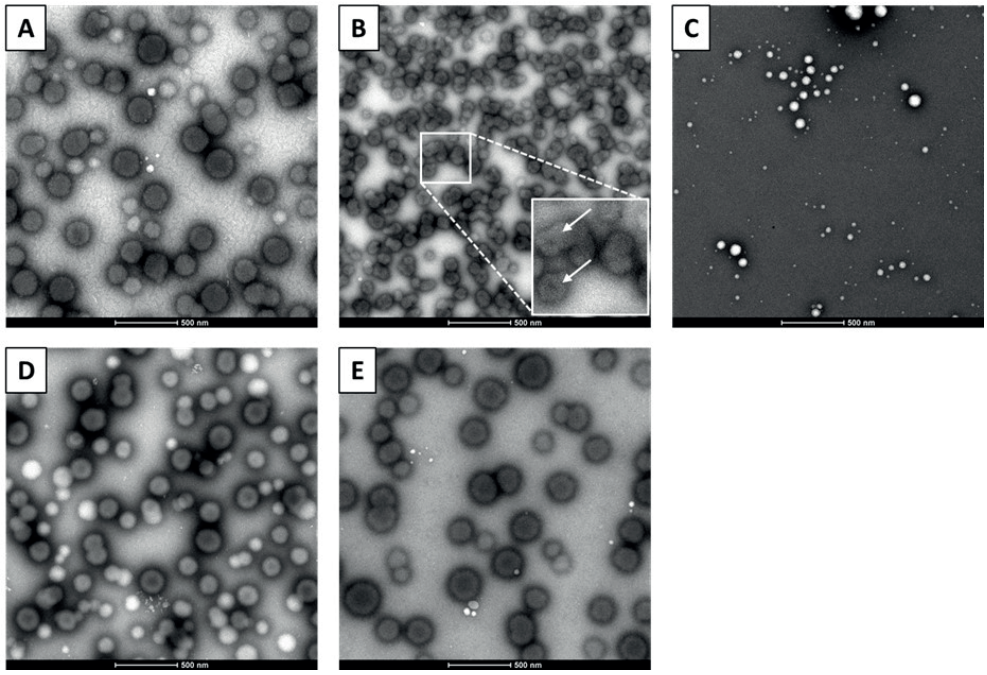

Figure 2. Transmission electron microscopy (TEM) of freshly produced Ab-Cath nanogels compared to redispersed nanogels upon lyophilization without cryoprotectants or in presence of PVA, dextran-40 or mannitol. (a) fresh nanogels, (b) nanogels lyophilized without cryoprotectant (white arrows in zoom-in indicate collapsed nanogels), (c) nanogels lyophilized with 10 mg/mL polyvinyl alcohol, (d) nanogels lyophilized with 10 mg/mL dextran-40 and (e) nanogels lyophilized with 50 mg/mL mannitol. Scale bar indicates 500 nm.

Table 3. Physicochemical properties of lyophilized and redispersed Ab-Cath nanogels.

Lyophilized, Cryoprotectant	Size (nm)	PDI	ZP (mV)	EE (%)	DL (%)
No	160 ± 7	0.08 ± 0.03	-19.7 ± 2.3	100.0 ± 0.0	23.0 ± 0.0
Yes, none	280 ± 99	0.17 ± 0.08	-24.8 ± 2.3	98.9 ± 1.1	22.9 ± 0.2
Yes, 50 mg/mL mannitol	205 ± 31	0.17 ± 0.02	-20.3 ± 3.1	96.8 ± 4.1	22.5 ± 0.7
Yes, 10 mg/mL PVA	261 ±28	0.17 ± 0.03	-25.5 ± 0.8	84.4 ± 5.9	20.2 ± 1.1
Yes, 10 mg/mL dextran-40	308 ± 71	0.24 ± 0.04	-23.0 ± 3.3	98.2 ± 1.6	22.8 ± 0.3

Nanogels were produced using 150 µg/mL Ab-Cath and 500 µg/mL OSA-HA. Data are presented as mean ± SD of three to four independent sample batch replicates. Abbreviations: OSA-HA = octenyl succinic anhydride-modified hyaluronic acid; PDI = polydispersity index; ZP = zeta potential; EE = encapsulation efficiency; DL = drug loading; PVA = polyvinyl alcohol.

3.5. Release of Ab-Cath from lyophilized and redispersed nanogels

The levels of Ab-Cath released from OSA-HA nanogels redispersed in PBS after lyophilization in presence of PVA or dextran-40 gradually increased until maximum values amounted to 48% and 36% at 25 h, respectively (**Figure 3**). Ab-Cath solution rapidly diffused through the dialysis membrane, reaching its maximum at around 25 h (**Figure S4**).

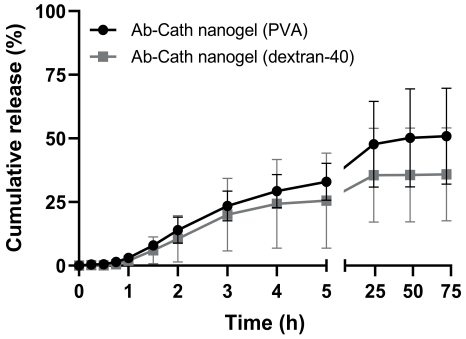

Figure 3. Release of Ab-Cath from PVA- or dextran-40-lyophilized OSA-HA nanogels. Release of Ab-Cath from OSA-HA nanogels in PBS at 37 °C. Data are presented as mean ± SD of 3 independent experiments and percentages are relative to the theoretical amount loaded.

3.6. Antimicrobial activities of lyophilized and redispersed Ab-Cath nanogels

The bactericidal activity of lyophilized and redispersed Ab-Cath nanogels against planktonic AMR *S. aureus* and *A. baumannii* in 50% (v/v) human plasma and against *E. coli* in 50% (v/v) urine was similar to that of Ab-Cath (**Table 4**). In addition, the antibiofilm activities of lyophilized Ab-Cath nanogels and Ab-Cath on AMR *S. aureus* and *A. baumannii* biofilms were also comparable. Of note, placebo nanogels and cryoprotectant solutions did not show any antibacterial activity at the tested concentrations (data not shown). Together, Ab-Cath nanogels were similarly effective as Ab-Cath solution against AMR bacteria.

Table 4. *In vitro* killing activities of lyophilized Ab-Cath nanogels.

	Growth state	$LC_{99.9}$ or $BEC_{99.9}$ (μM)			
		Ab-Cath	Ab-Cath nanogel	Ab-Cath nanogel	Ab-Cath nanogel
Cryoprotectant		-	-	PVA	dextran-40
S. aureus (LUH14616)	Planktonic	**3.2** (1.6-3.2)	**3.2** (3.2-6.4)	**6.4** (3.2-12.8)	**3.2** (3.2-12.8)
	24 h biofilm	**102.4** (51.2-204.8)	**51.2** (51.2->204.8)	**102.4** (51.2-204.8)	**102.4** (51.2-204.8)
A. baumannii (RUH875)	Planktonic	**0.8** (0.4-0.8)	**1.6** (0.2->3.2)	**0.8** (0.2-3.2)	**0.8** (0.2-3.2)
	24 h biofilm	**51.2** -	**51.2** -	**51.2** -	**51.2** -
E. coli (LUH15174)	Planktonic	**0.8** (0.2-0.8)	**3.2** (0.2->3.2)	**0.2** (0.2-0.8)	**0.8** (0.4-0.8)

The antibacterial activity of lyophilized Ab-Cath nanogels and Ab-Cath solution was assessed after 4 h exposure of AMR bacteria in 50% plasma (or urine in case of *E. coli*). Similarly, their antibiofilm activity against 24 h biofilms was determined after a 4 h exposure in PBS. Results are expressed as median and ranges of three to four independent experiments performed in duplicate and are shown as $LC_{99.9}$, i.e. the lowest concentration of peptide necessary to kill 99.9% of the planktonic bacteria, or as $BEC_{99.9}$, i.e. the lowest concentration of peptide necessary to kill 99.9% of the biofilm-residing bacteria. Ab-Cath nanogels were lyophilized without cryoprotectant, with 10 mg/mL polyvinyl alcohol (PVA) or 10 mg/mL dextran-40.

3.7. Decreased cytotoxicity to human primary skin fibroblasts of lyophilized and redispersed Ab-Cath nanogels

Next, the cytotoxic activities of lyophilized Ab-Cath nanogels redispersed in culture medium supplemented with 0.5% (v/v) human serum were compared to that of Ab-Cath by exposing monolayers of human primary skin fibroblasts for 4 h to these solutions. The EC_{50} of Ab-Cath for human primary skin fibroblasts amounted to 49 μM, while the EC_{50} values for Ab-Cath nanogels lyophilized without cryoprotectants or in presence of PVA or dextran-40 were 175 μM, 540 μM and 630 μM, respectively (**Figure 4a**). In agreement, Ab-Cath reduced the metabolic activity of these cells at considerably lower concentrations than Ab-Cath nanogels (**Figure 4b**). Placebo nanogels did not induce cytotoxicity in skin fibroblasts (**Figure S5**).

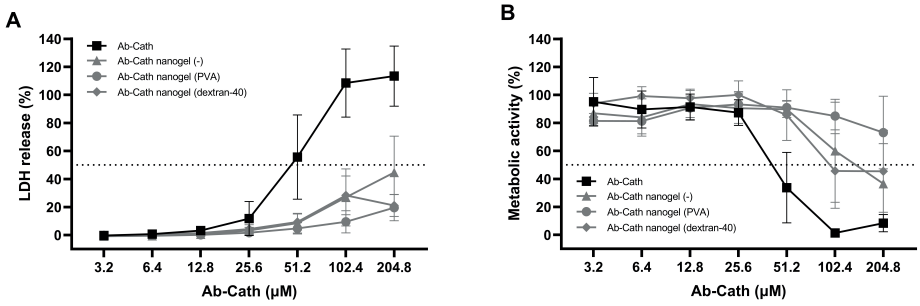

Figure 4. Cytotoxic activities of lyophilized Ab-Cath nanogels towards human primary skin fibroblasts. (a) LDH release and (b) metabolic activity measured by WST assay. Data are presented as mean ± SD of 2-3 experiments performed in duplicate.

3.8. Improved selectivity index of lyophilized and redispersed Ab-Cath nanogels

Comparison of the selectivity indexes, i.e. ratio between cytotoxicity and bactericidal or antibiofilm activity, revealed that loading in nanogels improved the overall selectivity index of Ab-Cath (**Table 5**). In addition, the selectivity indexes of Ab-Cath nanogels lyophilized in the presence of cryoprotectants were >1.5-fold higher than those of Ab-Cath nanogels lyophilized without cryoprotection. These data indicate that nanogel encapsulation of Ab-Cath allows the use of higher Ab-Cath concentrations without inducing cytotoxicity compared to Ab-Cath in solution. Overall, Ab-Cath nanogels lyophilized in presence of dextran-40 showed the most promising selectivity index for both planktonic and biofilm-residing AMR bacterial strains and was selected for further testing.

Table 5. Selectivity index of lyophilized Ab-Cath nanogels compared to Ab-Cath in solution.

	Growth state	Ab-Cath	Selectivity index Ab-Cath nanogel	Ab-Cath nanogel	Ab-Cath nanogel
Cryoprotectant		-	-	PVA	dextran-40
S. aureus (LUH14616)	Planktonic	15.3	54.6	84.4	197.0
	24 h biofilm	0.3	3.4	5.3	6.2
A. baumannii (RUH875)	Planktonic	61.3	109.3	674.9	788.0
	24 h biofilm	1.0	3.4	10.5	12.3
E. coli (LUH15174)	Planktonic	61.3	54.6	2699.5	788.0

The selectivity index of Ab-Cath solution and lyophilized Ab-Cath nanogels was calculated as median cytotoxicity IC_{50} value against human primary skin fibroblasts divided by median antimicrobial $LC_{99.9}$ or $BEC_{99.9}$ value towards AMR *S. aureus*, *A. baumannii* or *E. coli*. Ab-Cath nanogels were lyophilized without cryoprotectant or with either 10 mg/mL polyvinyl alcohol (PVA) or 10 mg/mL dextran-40.

3.9. Lyophilized and redispersed Ab-Cath nanogels maintained effectivity against AMR infections in a 3D human epidermal model, while they reduced cytotoxicity

Lastly, the efficacy of redispersed Ab-Cath nanogels lyophilized in the presence of dextran-40 and Ab-Cath were assessed against AMR *S. aureus* and *A. baumannii* colonizing a 3D human epidermal model. Results revealed a dose-dependent reduction in *S. aureus* and *A. baumannii* counts on the epidermal model upon exposure to Ab-Cath nanogels as well as to Ab-Cath solution (**Figure 5a,b**). Exposure of the bacteria on the epidermal model to placebo nanogels was without effect on bacterial counts. Furthermore, the highest dose of Ab-Cath induced minor cytotoxicity towards the epidermal model, which was significantly higher ($p=0.0288$) than Ab-Cath nanogels in the supernatant (**Figure 5c**), but this difference was not significant in the subnatant (**Figure 5d**).

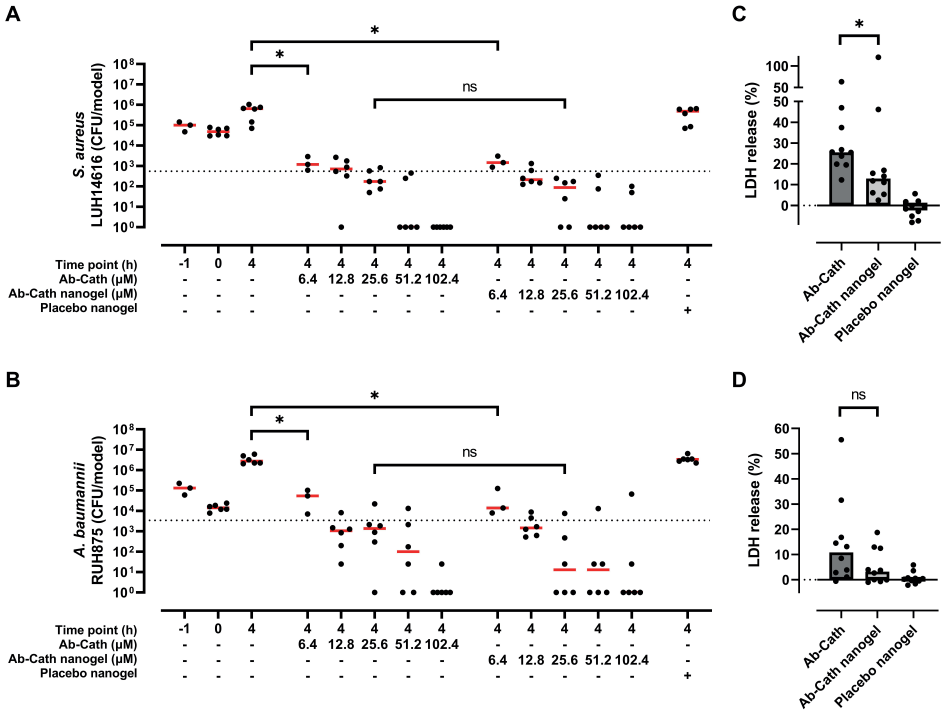

Figure 5. Bactericidal and cytotoxic effects of Ab-Cath nanogels lyophilized with dextran-40 compared to Ab-Cath in solution in a colonized 3D human epidermal model. Bactericidal effects were determined against adherent bacteria in 3D human skin equivalents colonized with (a) *S. aureus* and (b) *A. baumannii*, with dashed line indicating the $LC_{99.9}$. Cytotoxic effects to the 3D human skin equivalents were determined by measuring LDH release from the cells in the (c) supernatant and (d) subnatant, when exposed to a dose of 102.4 μM Ab-Cath. The amount of the placebo nanogel was equal to that for the highest dose of peptide. Data are shown as median and individual values of at least 3 experiments performed in duplicate. Statistical differences between 2 groups are depicted as ns for $p>0.05$ and * for $p\leq0.05$ as calculated by the Mann-Whitney U-test.

4. Discussion

The present study demonstrates that the snake cathelicidin Ab-Cath can be efficiently encapsulated in OSA-HA nanogels with favorable physicochemical properties. This conclusion is based on the following findings. First, we produced nanogels encapsulating 150 μg/mL Ab-Cath ranging from 156-232 nm in size with very homogenous distribution, as evidenced by the low polydispersity index (PDI=0.06) and by TEM. These results support previous observations that nanogel preparation by means of microfluidic-assisted self-assembly allows for a precise control over the self-assembly process of nanogels [18]. Moreover, these nanogel sizes met our intended size range of 150-200 nm, which was based on previous observations that transport across biofilms is negatively correlated to nanogels with increasing size [17] and nanogels in this size range are less likely to be removed by immune cells and the complement system [16]. Second, Ab-Cath nanogels

showed an overall reduction in the surface electro-negative net charge (-16.5 mV) compared to non-loaded nanogels (-32.6 mV), suggesting that in addition to being encapsulated in the nanogel this cationic peptide also binds to the nanogel's surface. Third, the encapsulation efficiency of Ab-Cath in OSA-HA nanogels was very high (>99%) in comparison to that of the antibiofilm peptide DJK-5-loaded and peptoid-loaded OSA-HA nanogels [10, 11]. This is likely related to intrinsic properties of the AMP, such as length [19], hydrophobicity [20] and charge [21]. In addition, loading of Ab-Cath into nanogels amounted to 23%, which is substantially higher than the <10% drug loading achieved for most existing nanomedicines [22]. This finding further emphasizes the potential of OSA-HA nanogels as high peptide drug-loading nanomedicine. Fourth, both Ab-Cath and non-loaded OSA-HA nanogels were physically stable over 15 days when stored at 4°C in ultrapure water. This is in agreement with previous observations that nanogel dispersions with a ZP of 10-30 mV above or below zero are considered relatively to highly stable [23]. Finally, we found that 26-33% of Ab-Cath was released from the lyophilized nanogels upon redispersion in the first 5 h followed by a sustained release phase over at least 72 h. This release is slower than the release of DJK-5 from OSA-HA nanogels in 24 h [11], but similar to the release of novicidin from OSA-HA nanogels in 14 days [9], indicating that the release profile is peptide-specific. Sustained release is favorable in treatment of complex wound and burn infections, as it minimizes the frequency of painful wound dressing changes [24]. The release of Ab-Cath from OSA-HA nanogels stabilizes after 72 h, indicating a slow sustained release phase and/or strong electrostatic interactions between cationic Ab-Cath and anionic OSA-HA polymer. The release rate is influenced by i) pH, ii) presence of degrading enzymes and iii) salt concentration [7]. Therefore, these release percentages should not be directly translated to concentrations used in the *in vitro* studies, where nanogels are used at varying conditions.

Lyophilization was used to concentrate Ab-Cath nanogels and for long-term storage, which are both essential for further development of these nanogels as therapeutics. However, this study showed that lyophilization without a cryoprotectant damaged the nanogels, affected their size and ZP, and resulted in poor antibacterial activities of Ab-Cath nanogels. Potential factors contributing to destabilization of the nanogels during lyophilization are related to the stress of freezing, dehydration and rehydration processes. We found that addition of cryoprotectants PVA or dextran-40 prior to lyophilization proved to fully abolish these drawbacks when lyophilizing the nanogels. Effective cryoprotectant concentrations of 10 mg/mL (=5% w/v) used in this study corroborate with concentrations used in previous studies: ≥5% (w/v) of mannitol [25], 1% (w/v) dextran-70 [26], ≥5% (w/v) dextran-90 [25] and ≥5% (w/v) of PVA [27]. To

the authors knowledge, this is the first report on successful lyophilization of AMP-loaded OSA-HA nanogels.

Importantly, this study confirms that encapsulation of Ab-Cath in OSA-HA nanogels is a successful strategy to reduce cytotoxicity and maintain antimicrobial activity of Ab-Cath, thus improving its selectivity index. This conclusion is based on the following findings. Encapsulation of Ab-Cath in OSA-HA nanogels lyophilized in presence of cryoprotectants PVA or dextran-40 maintained antimicrobial activity against planktonic AMR *S. aureus*, *A. baumannii* and *E. coli* and biofilm-residing AMR *S. aureus* and *A. baumannii*, while cytotoxicity for human primary skin fibroblasts was reduced 11- to 13-fold. The maintained activities combined with reduced cytotoxicity of Ab-Cath nanogels could potentially be attributed to i) partial shielding of Ab-Cath's cationic charge, such that Ab-Cath maintains its specificity for bacterial membranes but reduces its affinity to mammalian membranes, ii) desensitization of the human fibroblasts to increasing Ab-Cath concentrations due to the slow release of Ab-Cath from nanogels and/or, iii) synergistic effects of Ab-Cath and OSA-HA polymer thus increasing the activity of Ab-Cath at lower non-cytotoxic concentrations released from the nanogels in the first few hours. Moreover, lyophilized Ab-Cath nanogels were as effective upon redispersion as Ab-Cath in eliminating AMR *S. aureus* and *A. baumannii* colonizing a 3D human epidermal model, while minor cytotoxicity of Ab-Cath in this epidermal model was not found for the formulated peptide. Future efficacy testing of Ab-Cath nanogels and peptide solution should include *ex vivo* skin and/or animal models. Nevertheless, based on this study it can be concluded that Ab-Cath is an excellent antimicrobial to treat AMR bacteria, either planktonic, biofilm-residing or hiding in the wounded skin.

5. Conclusions

In summary, Ab-Cath was efficiently encapsulated in OSA-HA nanogels with excellent physicochemical and functional properties. In addition, a successful method to lyophilize Ab-Cath nanogels was developed, allowing for long term storage and concentration of the nanogels. Furthermore, the Ab-Cath nanogels were successful in eliminating bacteria when cutaneously applied on bacterial colonized 3D human skin. Together, OSA-HA nanogels are promising as delivery system for the snake cathelicidin Ab-Cath to combat AMR bacteria.

Author contributions

Conceptualization, M.E.v.G., S.N.K., M.A., R.I.K., J.W.D. and P.H.N.; methodology, M.E.v.G., S.N.K., M.A. and P.H.N.; validation, M.E.v.G., M.S., B.R.v.D. and E.B.; formal analysis, M.E.v.G. and M.S.; investigation, M.E.v.G., S.N.K., M.S., B.R.v.D. and E.B.; resources, B.R.v.D., R.I.K., J.W.D., H.M.N. and P.H.N.; writing—original

draft preparation, M.E.v.G., S.N.K. and P.H.N.; writing—review and editing, M.E.v.G., S.N.K., M.A., H.M.N. and P.H.N.; visualization, M.E.v.G.; supervision, M.E.v.G., S.N.K. and P.H.N.; project administration, P.H.N.; funding acquisition, P.H.N. All authors have read and agreed to the published version of the manuscript.

Funding

The authors acknowledge financial support from the Dutch Research Council (NWO), Novel Antibacterial Compounds and Therapies Antagonizing Resistance Program: grant number 16434. S.N.K. and H.M.N. were supported by the Novo Nordisk Foundation, Grand Challenge Program: NNF16OC0021948.

Informed consent statement

All human primary skin fibroblasts used in this study were isolated from surplus skin collected according to article 467 of the Dutch Law on Medical Treatment Agreement and the Code for Use of Human Tissue of the Dutch Federation of Biomedical Scientific Societies. The Declaration of Helsinki principles were followed when working with human primary cells.

Conflicts of interest

The authors declare no conflict of interest. The funders had no role in the design of the study; in the collection, analyses, or interpretation of data; in the writing of the manuscript, or in the decision to publish the results.

References

1. Kadam S, Nadkarni S, Lele J, Sakhalkar S, Mokashi P, Kaushik KS. Bioengineered Platforms for Chronic Wound Infection Studies: How Can We Make Them More Human-Relevant? Front Bioeng Biotechnol. 2019;7:418.
2. Serra R, Grande R, Butrico L, Rossi A, Settimio UF, Caroleo B, et al. Chronic wound infections: the role of Pseudomonas aeruginosa and Staphylococcus aureus. Expert Rev Anti Infect Ther. 2015;13(5):605-13.
3. Costerton JW, Lewandowski Z, Caldwell DE, Korber DR, Lappin-Scott HM. Microbial biofilms. Annu Rev Microbiol. 1995;49:711-45.
4. Mah TF. Biofilm-specific antibiotic resistance. Future Microbiol. 2012;7(9):1061-72.
5. Drago L, Cappelletti L, De Vecchi E, Pignataro L, Torretta S, Mattina R. Antiadhesive and antibiofilm activity of hyaluronic acid against bacteria responsible for respiratory tract infections. APMIS. 2014;122(10):1013-9.
6. Eenschooten C, Guillaumie F, Kontogeorgis GM, Stenby EH, Schwach-Abdellaoui KJCP. Preparation and structural characterisation of novel and versatile amphiphilic octenyl succinic anhydride–modified hyaluronic acid derivatives. 2010;79(3):597-605.
7. Kabanov AV, Vinogradov SV. Nanogels as Pharmaceutical Carriers: Finite Networks of Infinite Capabilities. Angew Chem Int Edit. 2009;48(30):5418-29.
8. Nordstrom R, Malmsten M. Delivery systems for antimicrobial peptides. Adv Colloid Interface Sci. 2017;242:17-34.
9. Water JJ, Kim Y, Maltesen MJ, Franzyk H, Foged C, Nielsen HM. Hyaluronic Acid-Based Nanogels Produced by Microfluidics-Facilitated Self-Assembly Improves the Safety Profile of the Cationic Host Defense Peptide Novicidin. Pharm Res. 2015;32(8):2727-35.
10. Klodzinska SN, Molchanova N, Franzyk H, Hansen PR, Damborg P, Nielsen HM. Biopolymer nanogels improve antibacterial activity and safety profile of a novel lysine-based alpha-peptide/beta-peptoid peptidomimetic. Eur J Pharm Biopharm. 2018;128:1-9.
11. Klodzinska SN, Pletzer D, Rahanjam N, Rades T, Hancock REW, Nielsen HM. Hyaluronic acid-based nanogels improve in vivo compatibility of the anti-biofilm peptide DJK-5. Nanomedicine. 2019;20:102022.
12. Daoud-Mahammed S, Couvreur P, Gref R. Novel self-assembling nanogels: stability and lyophilisation studies. Int J Pharm. 2007;332(1-2):185-91.
13. Abdelwahed W, Degobert G, Stainmesse S, Fessi H. Freeze-drying of nanoparticles: Formulation, process and storage considerations. Adv Drug Deliver Rev. 2006;58(15):1688-713.
14. Kim Y, Lee Chung B, Ma M, Mulder WJ, Fayad ZA, Farokhzad OC, et al. Mass production and size control of lipid-polymer hybrid nanoparticles through controlled microvortices. Nano Lett. 2012;12(7):3587-91.
15. van Gent ME, van der Reijden TJK, Lennard PR, de Visser AW, Schonkeren-Ravensbergen B, Dolezal N, et al. Synergism between the Synthetic Antibacterial and Antibiofilm Peptide (SAAP)-148 and Halicin. Antibiotics-Basel. 2022;11(5).
16. Hoshyar N, Gray S, Han H, Bao G. The effect of nanoparticle size on in vivo pharmacokinetics and cellular interaction. Nanomedicine (Lond). 2016;11(6):673-92.
17. Peulen TO, Wilkinson KJ. Diffusion of nanoparticles in a biofilm. Environ Sci Technol. 2011;45(8):3367-73.
18. Capretto L, Cheng W, Hill M, Zhang XL. Micromixing Within Microfluidic Devices. Top Curr Chem. 2011;304:27-68.
19. Nystrom L, Nordstrom R, Bramhill J, Saunders BR, Alvarez-Asencio R, Rutland MW, et al. Factors Affecting Peptide Interactions with Surface-Bound Microgels. Biomacromolecules. 2016;17(2):669-78.
20. Bysell H, Ransson P, Schmidtchen A, Malmsten M. Effect of Hydrophobicity on the Interaction between Antimicrobial Peptides and Poly(acrylic acid) Microgels. J Phys Chem B. 2010;114(3):1307-13.
21. Mansson R, Bysell H, Hansson P, Schmidtchen A, Malmsten M. Effects of peptide secondary structure on the interaction with oppositely charged microgels. Biomacromolecules. 2011;12(2):419-24.

22. Shen S, Wu Y, Liu Y, Wu D. High drug-loading nanomedicines: progress, current status, and prospects. Int J Nanomedicine. 2017;12:4085-109.
23. Bhattacharjee S. DLS and zeta potential - What they are and what they are not? J Control Release. 2016;235:337-51.
24. van Gent ME, Ali M, Nibbering PH, Klodzinska SN. Current Advances in Lipid and Polymeric Antimicrobial Peptide Delivery Systems and Coatings for the Prevention and Treatment of Bacterial Infections. Pharmaceutics. 2021;13(11).
25. Chacon M, Molpeceres J, Berges L, Guzman M, Aberturas MR. Stability and freeze-drying of cyclosporine loaded poly(D,L lactide-glycolide) carriers. Eur J Pharm Sci. 1999;8(2):99-107.
26. Roy D, Guillon X, Lescure F, Couvreur P, Bru N, Breton P. On shelf stability of freeze-dried poly(methylidene malonate 2.1.2) nanoparticles. Int J Pharm. 1997;148(2):165-75.
27. Abdelwahed W, Degobert G, Fessi H. A pilot study of freeze drying of poly(epsilon-caprolactone) nanocapsules stabilized by poly(vinyl alcohol): formulation and process optimization. Int J Pharm. 2006;309(1-2):178-88.

Supplementary materials

Supplementary Methods

^{1}H-NMR analysis

The purity and degree of substitution (DS) was investigated by ^{1}H-NMR. OSA-HA (8 mg) was dissolved in D_2O (0.8 mL) and stirred for 1 hour at room temperature. The solution was transferred to a glass NMR tube. The NMR spectra were recorded on an Agilent-400 MR DD2 (399.67 MHz for ^{1}H-NMR) in D_2O at 298 K. The chemical shift values are given in ppm and J values in Hz. The DS is determined by comparing the number of protons of the terminal CH_3-group of the octenyl groups (0.9 ppm) to that of the terminal methyl amides on native HA (2.0 ppm). The spectra of native HA and of OSA–HA were assigned based on previous reports [1-3].

Supplementary Figures

Rate of substitution of OSA to HA polymer

HA polymer was substituted with OSA during a one-step synthesis. ^{1}H-NMR analysis of produced OSA-HA polymer revealed that HA polymer (**Figure S1**) was substituted with OSA with a rate of 17% (**Figure S2**) or 32% (**Figure S3**) based on intensity per proton of singlet peak at 1.8-2.0 ppm compared to singlet peak at 0.7-0.9 ppm.

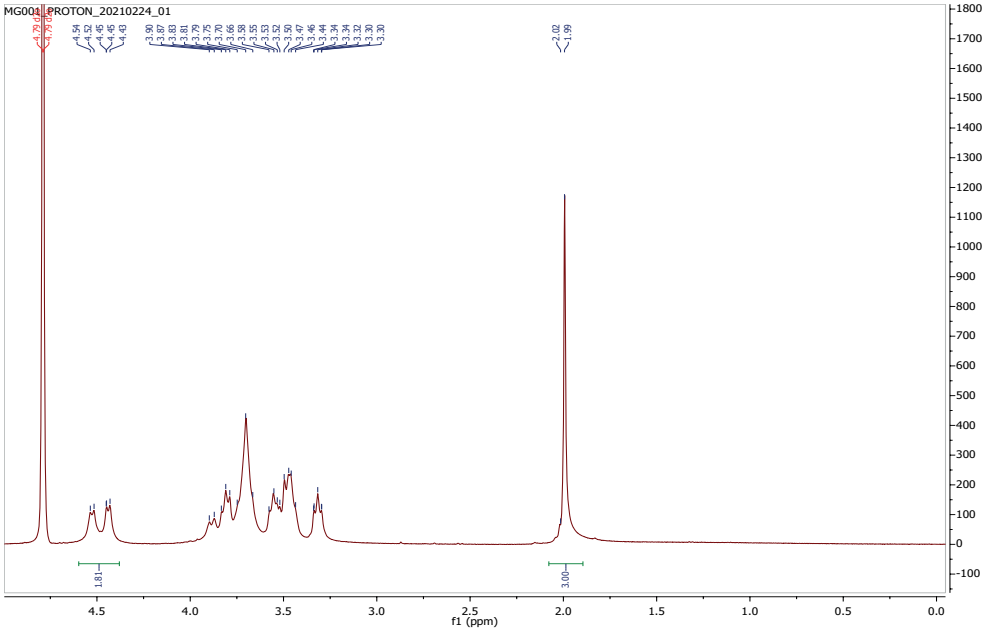

Figure S1. ^{1}H-NMR of HA polymer.

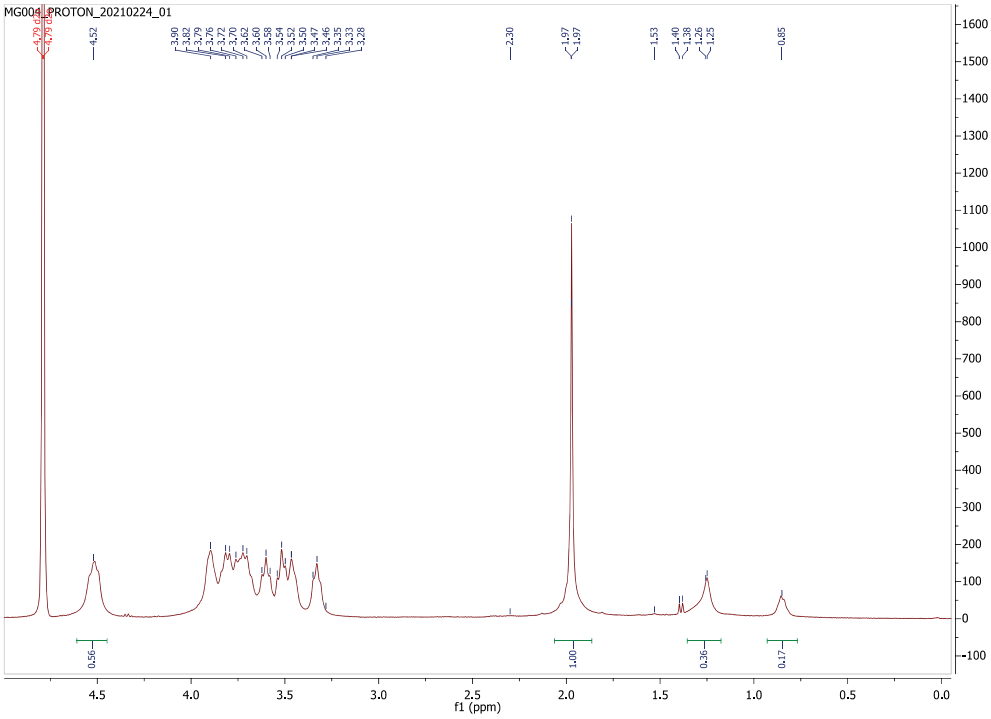

Figure S2. ^{1}H-NMR of OSA-HA polymer with a rate of substitution of 17%.

Effect of cryoprotectant and its concentration on physicochemical properties of lyophilized Ab-Cath nanogels

Fresh nanogels were lyophilized in presence of cryoprotectants trehalose, mannitol, PVA or dextran-40 with concentrations ranging 5-50 mg/mL and physicochemical properties (size, PDI and ZP) of lyophilized nanogels redispersed in ultrapure water were determined (**Table S1**). Lyophilization with increasing amounts of trehalose, mannitol or the combination trehalose and mannitol resulted in decreased nanogel sizes. For these cryoprotectants the highest concentration of 50 mg/mL resulted in nanogels with most optimal physicochemical properties, with mannitol reaching the lowest nanogel size of 236 nm. Lyophilization with increasing amounts of PVA or dextran-40 resulted in increased nanogel sizes. For these cryoprotectants the lower concentration of 10 mg/mL resulted in nanogels with most optimal physicochemical properties, with 255 nm and 282 nm for PVA and dextran-40, respectively. Therefore, further studies were conducted with nanogels lyophilized with 50 mg/mL mannitol, 10 mg/mL PVA or 10 mg/mL dextran-40.

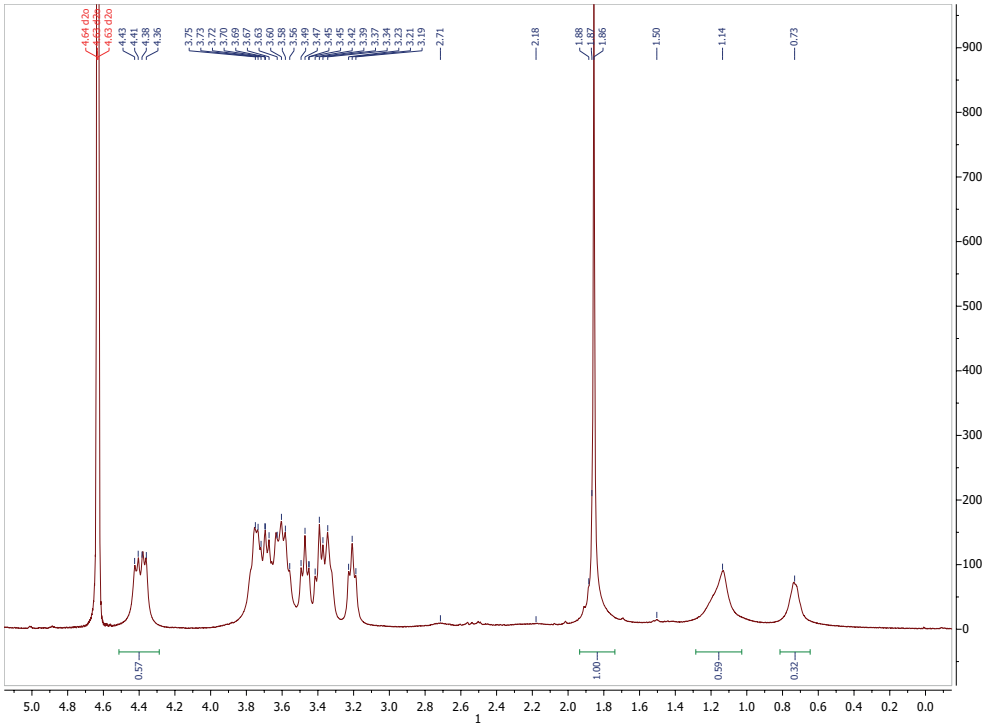

Figure S3. ^{1}H-NMR of OSA-HA polymer with a rate of substitution of 32%.

Table S1. Effects of cryoprotectants on physicochemical properties of lyophilized Ab-Cath nanogels.

Cryoprotectant	Cryoprotectant (mg/mL)	Size (nm)	PDI	ZP (mV)	Replicates
Trehalose	10	1063	0.61	-22.0	1
Trehalose	25	857	0.42	-21.4	1
Trehalose	50	330	0.35	-20.0	1
Mannitol	10	591 ± 8	0.44 ± 0.04	-22.3 ± 0.4	2
Mannitol	25	333 ± 1	0.27 ± 0.08	-20.9 ± 1.6	2
Mannitol	50	236 ± 29	0.17 ± 0.02	-20.3 ± 3.1	4 or 5
Trehalose & mannitol	10 & 10	724	0.50	-22.9	1
Trehalose & mannitol	25 & 25	401	0.21	-20.4	1
Trehalose & mannitol	50 & 50	300	0.25	-18.6	1
PVA	5	255	0.15	-30.1	1
PVA	10	255 ± 28	0.17 ± 0.03	-24.6 ± 2.5	5
PVA	25	370 ± 8	0.22 ± 0.01	-19.0 ± 0.2	2
PVA	50	634	0.26	-12.9	1
Dextran-40	5	282	0.20	-29.0	1
Dextran-40	10	309 ± 58	0.24 ± 0.04	-23.0 ± 3.3	4
Dextran-40	25	305 ± 9	0.24 ± 0.01	-19.1 ± 0.6	2
Dextran-40	50	496	0.27	-15.6	1

Lyophilized nanogels contain 150 µg/mL Ab-Cath and 500 µg/mL OSA-HA. Data are presented as mean ± standard deviation of one to five independent sample batch replicates. Abbreviations: OSA-HA = octenyl succinic anhydride-modified hyaluronic acid; PDI = polydispersity index; ZP = zeta potential; PVA = polyvinyl alcohol.

Diffusion rate of Ab-Cath solution through dialysis membrane

Ab-Cath solution was included as intrinsic control for the release study using dialysis membranes. Results showed complete diffusion of Ab-Cath through the dialysis membrane within 25 h (**Figure S4**).

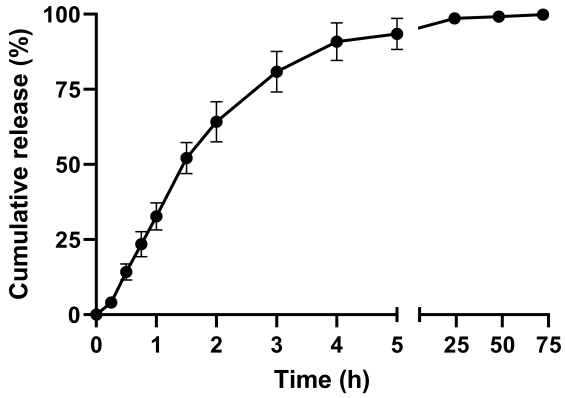

Figure S4. Diffusion profile of Ab-Cath through the dialysis membrane. Diffusion of Ab-Cath from solution in PBS at 37°C using float-a-lyzer dialysis method. Data are presented as mean ± SD of three independent experiments.

Placebo lyophilized nanogels did not induce cytotoxic activities towards human primary skin fibroblasts

The cytotoxic activity of lyophilized and redispersed placebo nanogels on monolayers of human primary skin fibroblasts upon 4 h exposure in culture medium supplemented with 0.5% (v/v) human serum was included at polymer concentrations equal to those at specific Ab-Cath concentrations. Results revealed that the placebo nanogels at these concentrations did not induce LDH release by the cells, while metabolic activity was reduced slightly, already at the lower concentrations and without prominent dose-response effects (**Figure S5**).

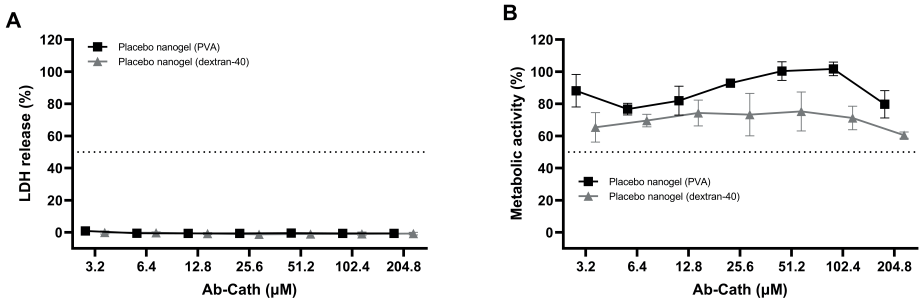

Figure S5. Cytotoxic activities of lyophilized placebo nanogels towards human primary skin fibroblasts. (a) LDH release and (b) metabolic activity measured by WST assay. Data are presented as means with standard deviation of one experiment performed in duplicate. Placebo nanogels were lyophilized with 10 mg/mL polyvinyl alcohol (PVA) or 10 mg/mL dextran-40.

Supplementary materials references

1. Eenschooten, C., et al., Preparation and structural characterisation of novel and versatile amphiphilic octenyl succinic anhydride–modified hyaluronic acid derivatives. 2010. 79(3): p. 597-605.
2. Pretsch, E., et al., Structure determination of organic compounds. Vol. 13. 2009: Springer.
3. Welti, D., D.A. Rees, and E.J. Welsh, Solution Conformation of Glycosaminoglycans - Assignment of the 300-Mhz H-1 Magnetic Resonance-Spectra of Chondroitin 4-Sulfate, Chondroitin 6-Sulfate and Hyaluronate, and Investigation of an Alkali-Induced Conformation Change. European Journal of Biochemistry, 1979. 94(2): p. 505-514.